AFRL-RY-HS-TR-2008-0022

TERAHERTZ PLASMON-INDUCED CONDUCTANCE EFFECTS IN SEMICONDUCTOR HETEROSTRUCTURES

Robert E. Peale

University of Central Florida
Department of Physics
4000 Central Florida Blvd.
Orlando FL 32816

Final Report

5 September 2008

AIR FORCE RESEARCH LABORATORY
Sensors Directorate
Electromagnetics Technology Division
Hanscom AFB MA 01731-2909

NOTICE AND SIGNATURE PAGE

Using Government drawings, specifications, or other data included in this document for any purpose other than Government procurement does not in any way obligate the U.S. Government. The fact that the Government formulated or supplied the drawings, specifications, or other data does not license the holder or any other person or corporation; or convey any rights or permission to manufacture, use, or sell any patented invention that may relate to them.

This report was cleared for public release by the Electronic Systems Center Public Affairs Office for the Air Force Research Laboratory Electromagnetic Technology Division and is available to the general public, including foreign nationals. Copies may be obtained from the Defense Technical Information Center (DTIC) (http://www.dtic.mil).

AFRL-RY-HS-TR-2008-0022 HAS BEEN REVIEWED AND IS APPROVED FOR PUBLICATION IN ACCORDANCE WITH ASSIGNED DISTRIBUTION STATEMENT.

WALTER BUCHWALD
Contract Monitor
Optoelectronics Technology Branch

JOSEPH LORENZO
Chief, Optoelectronics Technology Branch
Electromagnetics Technology Division

MICHAEL N. ALEXANDER
Technical Advisor
Electromagnetic Technology Division

This report is published in the interest of scientific and technical information exchange, and its publication does not constitute the Government's approval or disapproval of its ideas or findings.

REPORT DOCUMENTATION PAGE

Form Approved
OMB No. 0704-0188

PLEASE DO NOT RETURN YOUR FORM TO THE ABOVE ADDRESS.

1. REPORT DATE *(DD-MM-YYYY)*	2. REPORT TYPE	3. DATES COVERED *(From - To)*
05-09-2008	Final Report	25 Jul 07 to 31 May 08

4. TITLE AND SUBTITLE
Terahertz Plasmon-Induced Conductance Effects in Semiconductor Heterostructures

5a. CONTRACT NUMBER
FA8718-07C-0036

5b. GRANT NUMBER

5c. PROGRAM ELEMENT NUMBER
62204F

6. AUTHOR(S)
Robert E. Peale

5d. PROJECT NUMBER
4916

5e. TASK NUMBER
HC

5f. WORK UNIT NUMBER
0C

7. PERFORMING ORGANIZATION NAME(S) AND ADDRESS(ES)
University of Central Florida
Department of Physics
4000 Central Florida Blvd.
Orlando FL 32816

8. PERFORMING ORGANIZATION REPORT NUMBER

9. SPONSORING/MONITORING AGENCY NAME(S) AND ADDRESS(ES)
Electromagnetics Technology Division
Sensors Directorate
Air Force Research Laboratory/RYHC
80 Scott Drive
Hanscom AFB, MA 01731-2909
Source Code 437890

10. SPONSOR/MONITOR'S ACRONYM(S)
AFRL-RY-HS

11. SPONSOR/MONITOR'S REPORT NUMBER(S)
AFRL-RY-HS-TR-2008-0022

12. DISTRIBUTION/AVAILABILITY STATEMENT
Approved for public release; distribution unlimited 66ABW-2008-0417

13. SUPPLEMENTARY NOTES

14. ABSTRACT
Experimental investigation of the coupling of free space radiation to surface plasmons by silver or Pd2Si gratings was performed for different grating profiles at CO2 laser wavelengths. Comparison of the results with the theory of Hessel and Oliner 1965 and of Wheeler, Arakawa, and Ritchie 1976 suggests that the former gives the more accurate description in the long-wave IR. For that theory, the comparison gives an empirical non-linear relation between the physical depth of the grating grooves and the surface-impedance modulation amplitude. The Hessel-Oliner theory predicts stronger photon-plasmon coupling for the higher impedance silicide, suggesting that these conductors may be preferable for silicon-based IR plasmonic devices. Shifts and broadening of the surface Plasmon resonances with increasing grating height are also reported and found to be weaker than similar effects observed previously at visible wavelengths.

15. SUBJECT TERMS
Surface Plasmon, permittivity, Palladium Silicide, terahertz, far infrared

16. SECURITY CLASSIFICATION OF:			17. LIMITATION OF ABSTRACT	18. NUMBER OF PAGES	19a. NAME OF RESPONSIBLE PERSON
a. REPORT	b. ABSTRACT	c. THIS PAGE			Walter Buchwald
Unclassified	Unclassified	Unclassified	SAR	25	19b. TELEPHONE NUMBER *(Include area code)* NA

TABLE OF CONTENTS

LIST OF FIGURES

LIST OF TABLES

1. Introduction

Gratings are a key component in proposed nanophotonic integrated circuits, where they are used to couple free electromagnetic waves into surface plasmon polaritons (SPP) and similarly for the reverse process as out-couplers. Much work remains in order to design and optimize such coupling structures for efficient conversion and to provide good beam-profiles [1]. This paper experimentally considers the effects of grating profile and surface impedance on the strength of the coupling. Results are compared with existing analytical theories to determine their predictive value in optimization efforts. Although most recent efforts in the study of surface plasmons have been concentrated in the visible and near IR range, we purposely choose to concentrate on the long-wave IR for reasons explained elsewhere [2].

Photon-SPP coupling for Ag sinusoidal gratings of different amplitudes has been studied experimentally in [3, 4]. In [3], SPPs were excited by electron beams, and the angular distribution of out-coupled photons was recorded. In [4], specular reflection from gratings vs. angle of incidence was measured, with dips appearing when light energy was converted to SPPs. Both studies were confined to visible frequencies. Both reported a shift to larger angles and a broadening of the resonance with increasing grating height. These changes were attributed to a dependence of the permittivity of the metal on surface morphology. In neither case were the angular spectra compared to theory.

Wheeler, Arakawa, and Ritchie [5] reported effects of grating groove morphology in an experiment similar to [4], but they additionally compared their results to calculations based on a perturbative theory of SPP generation probability. The experiment was confined to visible wavelengths, and the gratings were triangular with small blaze angles, amplitudes ~100 nm and periods ~1 μm. The agreement between theory and experiment was excellent.

This paper presents an experiment similar to those of [4, 5] but for rectangular grating profiles and at 10 μm wavelengths. Calculated angular resonance spectra using the theory of Hessel and Oliner [6] agree adequately with observations. We determine an empirical relation between the physical grating height and the amplitude of the

impedance modulation, an essential parameter in the Hessel-Oliner formalism. This relation is found to be non-linear.

Though agreement between experiment and the perturbative theory at visible wavelengths of Ref. [5] was excellent, and we can accurately reproduce their calculations, this theory agrees poorly with our observations in the long-wave IR, even though our grating amplitudes and periods, normalized to wavelength, are comparable to those of [5]. Thus, the theory of [5] appears less generally useful for SPP coupler optimization.

The Hessel-Oliner theory predicts an increased coupling of photons to SPPs when the surface impedance is increased. This supports silicides and other conductors with low carrier concentration as promising for silicon-based IR plasmonics [2]. To test this, measurements were performed on a Pd_2Si grating having parameters similar to the Ag ones. The silicide results are also adequately described by the Hessel-Oliner theory with an impedance modulation parameter compatible with values found for silver.

The observed shifts and broadening with grating height in the LWIR are smaller than observed in the visible range when the grating height is normalized to the free space wavelength. This suggests that LWIR photon-SPP couplers are more forgiving in regards to design tolerances when compared to visible wavelength couplers.

2. Experiment

Gratings with 20 periods were formed by evaporation of Ag through a mask on top of a 200 nm evaporated Ag film supported by a polished silicon substrate. The supporting Ag film is optically thick in the IR. The period of all gratings was 20 μm and the duty cycle was 50%, but the grating height was varied. Measured profiles determine the peak to peak height *h* of the gratings and confirm that the grating lines have sharp square edges.

The gratings were mounted and aligned on a motorized goniometer. Specular reflection of p-polarized CO_2 laser radiation was collected by a power meter P as a function of the angle of incidence, as indicated schematically in Fig. 1. Generation of SPPs was indicated by loss of power in the reflected beam for a narrow range of incidence angle.

Pd_2Si gratings were prepared as follows. A new 2-inch Si wafer was coated with ~600 nm Pd in an e-beam evaporator, than annealed for four hours at ~500°C with flowing nitrogen to form the silicide. Standard photolithography techniques were used along with an e-beam evaporator to deposit 600 nm of Pd form the grating bars. The wafer was annealed again at ~500°C in flowing nitrogen for 8 hours to complete the formation of the silicide grating. Step profilometer measurements reveal a final grating height of 0.67 μm.

To confirm the generation of propagating SPPs at the resonance angle, some samples were prepared with a second grating separated by 1 cm from the first, as indicated schematically in Fig. 1. An IR camera was set up to image this second grating, while all rays from the first grating were blocked by a screen from reaching the camera. With the goniometer, it was convenient to observe the m = 1 SPP, which outcouples in a direction parallel to the specularly reflected beam. No attempt was made to observe the other expected outcoupled beams.

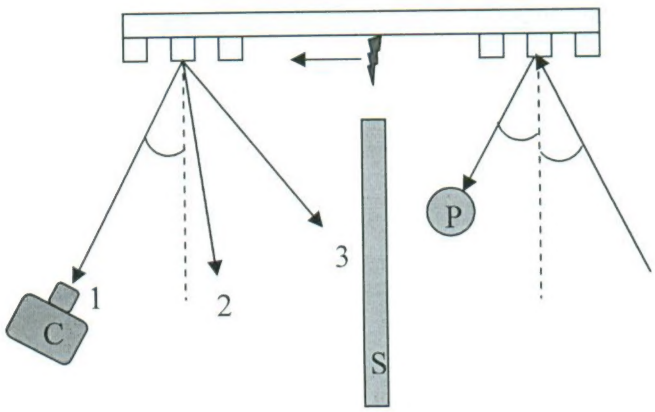

Figure 1 Schematic of experiment. P-polarized CO_2 laser radiation is incident on the right grating, and specular reflection is monitored as a function of angle of incidence using power meter P. A second grating 1 cm to the left outcouples the SPP that has traveled to it, and this event is imaged with an infrared camera C. The screen S prevents any rays from the first grating reaching the camera.

3. Theoretical Considerations

The theory of Hessel and Oliner [6] for Wood Anomalies, models the grating as a sinusoidally modulated surface impedance, $Z(x)$. For purposes of obtaining and testing

simple design formulas, we consider here only the first Fourier component of that modulation represented by

$$Z(x) = Z_0 \left(1 + M \, Cos\left[\frac{2\pi x}{d} \right] \right), \tag{1}$$

even though our actual gratings have rectangular ridges containing many higher harmonics. The effect of neglecting these higher harmonics is to eliminate SPP resonances with m > 1 from the calculated angular reflectance spectra. In Eq. (1), *M* is the modulation index (related to the depth of the grooves), and *d* is the period along the *x*-direction. The average surface impedance (or the limit for zero modulation) is given by

$$Z_0 = \sqrt{\frac{\mu_o}{(\varepsilon' + i\varepsilon'')\varepsilon_o}} = \frac{377\Omega}{\sqrt{\varepsilon' + i\varepsilon''}}, \tag{2}$$

where μ_0, ε_0 and 377 Ω are the permeability, permittivity, and impedance of free space, while ε' and ε'' are the real and imaginary parts of the relative permittivity for the metal, respectively. For metals in the infrared, we generally have the condition $\varepsilon'' << |\varepsilon'|$ and $\varepsilon' < 0$, giving for the *relative* surface impedance

$$\zeta \equiv \frac{Z_0}{377\Omega} \approx \frac{-i}{\sqrt{|\varepsilon'|}}. \tag{3}$$

If the imaginary part cannot be neglected, and assuming $\varepsilon' = -|\varepsilon'|$, we have

$$\zeta = -i \left(|\varepsilon'|^2 + \varepsilon''^2 \right)^{-1/4} \left\{ Cos\left[\phi/2 \right] + i \, Sin\left[\phi/2 \right] \right\} \tag{4}$$

where $\phi = Tan^{-1}(\varepsilon''/|\varepsilon'|)$. The permittivity values measured for our silver and Pd_2Si films is given in Table I, together with relative surface impedance values from Eqs. (3) and (4).

Table 1. Optical parameters of Ag and Pd_2Si.

	$\lambda(\mu m)$	$-\varepsilon'$	ε''	ζ(Eq. 3)	ζ (Eq. 4)
Ag	9.250	5397 ± 300	1463 ± 120	-i 0.0136	-i(0.0133 + i 0.0018)
	10.591	6774 ± 500	1971 ± 300	-i 0.0121	-i(0.0118 + i 0.0017)
Pd_2Si	9.250	527 ± 18	260 ± 14	-i 0.0436	-i(0.0402 + i 0.0094)
	10.591	713 ± 9	360 ± 9	-i 0.0374	-i(0.0344 + i 0.0082)

The magnetic field of the incident wave polarized in the xz plane of incidence is $H\ Exp[i(k_s x - \kappa_o z)]$, where the in-plane wavenumber, k_s, is related to the incidence angle by $k_s = k\ Sin(\theta)$. The field of the scattered wave is

$$H_S(x,z) = \sum_{n=-\infty}^{\infty} I_n\ Exp\left[i\left(k_s + \frac{2\pi n}{d} \right) x + i\kappa_n z \right] \tag{5}$$

where I_n are the complex amplitudes of the n^{th} spectral orders (propagating or not) and

$$\kappa_n = \sqrt{k^2 - \left(k_s + \frac{2\pi n}{d} \right)^2} \tag{6}$$

For sufficiently large n, κ_n is pure imaginary, the nth Fourier component is exponentially damped in the direction normal to the surface, and no refracted spectral order is present. Otherwise, κ_n is purely real giving the usual propagating spectral orders of the

grating. The vanishing of κ_n is known as the Rayleigh condition [7] for the occurrence of Wood's anomalies [8]. Here, propagating spectral orders either emerge or disappear, since $\kappa_n = 0$ is identical to the diffraction for $\theta_m = \pm 90$ deg, namely $Sin(\pm\pi/2) - Sin(\theta) = n\lambda/d$. The Rayleigh condition results in a redistribution of energy among the various orders, including the zeroth (specular) order I_0.

Our experiment measures specular reflection from the grating, for which the reflectivity is [6]

$$R = |I_0/H|^2 = \left| \frac{2D_0 - 4/M}{D_0 + A_1 + B_{-1}} - 1 \right|^2, \tag{7}$$

With

$$D_n = \frac{2}{M}\left[1 + \frac{\kappa_n}{\zeta k}\right], \tag{8}$$

$$A_1 = -\left\{D_1 - \left[D_2 - \left(D_3 - \ldots\right)^{-1}\right]^{-1}\right\}^{-1}, \tag{9}$$

$$B_{-1} = -\left\{D_{-1} - \left[D_{-2} - \left(D_{-3} - \ldots\right)^{-1}\right]^{-1}\right\}^{-1}, \tag{10}$$

Eqs. (9) and (10) are continued fractions. If at a certain angle D_1 or D_{-1} become small, the other D_n remain large, so that here we may approximate Eqs. (9) and (10) by $A_1 \approx -1/D_1$ and $B_{-1} \approx -1/D_{-1}$ leaving the following approximation for specular reflection

$$R \approx \left| \frac{2D_0 - 4/M}{D_0 + \frac{1}{D_1} - \frac{1}{D_{-1}}} \right|^2 \tag{11}$$

We find this approximation to be good throughout the angle range of our experiment. It seems clear at this point that the specular reflection from a grating is controlled by the behavior of the $D_{n\neq 0}$ terms. Considering only the n=1 term, clearly, at those conditions

for which D_1 reaches a minimum there will in general also be a specular reflection mimimium. To delve deeper, the behavior of $D_{n\neq 0}$ is determined by two complex values, namely, the relative surface impedance, ζ, and K_n. At some incident angle, $\theta = \theta_m$, K_n=0, and the diffracted beam is parallel to the grating surface. This corresponds to the Rayleigh condition for metal gratings. For values of θ such that $\theta < \theta_m$, K_n is always a real value and we have

$$\mathrm{Re}\left[D_1\right] = \frac{2}{M}\left[1 + \frac{\varsigma' |\kappa_n|}{|\varsigma|^2 k}\right] \tag{12}$$

And, because for metals $\varsigma'' = -|\varsigma''|$, we have

$$\mathrm{Im}\left[D_1\right] = \frac{2|\varsigma''||\kappa_n|}{M|\varsigma|^2 k} \quad . \tag{13}$$

Both terms are always positive and slowly varying which implies no resonance condition for $\theta < \theta_m$. For the case $\theta > \theta_m$, K_n is always imaginary, therefore K_n can be written as $\kappa_n = i|\kappa_n|$ provided

$$|\kappa_n| = \sqrt{\left(kSin\theta + \frac{2\pi}{d}\right)^2 - k^2} \quad . \tag{14}$$

This leads to the imaganary parts of D_1 as

$$\mathrm{Im}\left[D_1\right] = \frac{2\varsigma' |\kappa_n|}{|\varsigma|^2 k} \tag{15}$$

Which is always positive and the real part of D_1 as

$$\mathrm{Re}[D_1]=\frac{2}{M}\left[1-\frac{|\varsigma''|\kappa_n|}{|\varsigma|^2 k}\right]. \tag{16}$$

Equation (16) will go to zero, and the specular reflection will reach a minimum when the condition

$$1=\frac{|\varsigma''|\kappa_n|}{|\varsigma|^2 k} \tag{17}$$

Is met. This immediately leads to the resonance condition in terms of the relative surface impedance as

$$Sin(\theta)+\frac{\lambda}{d}=\sqrt{1+\frac{|\varsigma|^4}{[\mathrm{Im}(\varsigma)]^2}}\ . \tag{18}$$

To make clear the origin of resonance phenomena, we rewrite Eq. (7) as

$$R=\frac{(D_0'+A_1'+B_{-1}')^2+\left(\frac{4Cos(\theta)}{M|\varsigma|}-D_0''-A_1''-B_{-1}''\right)^2}{(D_0'+A_1'+B_{-1}')^2+(D_0''+A_1''+B_{-1}'')^2}. \tag{12}$$

The vanishing of D_1 causes a derivative-like resonance line shape in A_1' and an asymmetric peak in A_1'', while all other factors in Eq. (11) vary slowly with θ. This phenomenon is responsible for an asymmetric resonance feature in the specular reflectance R. When more terms are kept in the continued fractions (9) and (10), progressively weaker resonances can be observed whenever $D_n = 0$. The weakening of the resonances with increasing order results from the neglect of higher harmonics in the

Fourier expansion of the grating Eq. (1), but including these harmonics results in a much more complicated formula for R. Consequently, we limit our discussion to the m = 1 resonance.

The vanishing of D_1' with the assumptions $\varepsilon' < 0$ and $|\varepsilon'| >> \varepsilon'' >> 1$ gives a condition for the generation of a "guided surface wave" [6] of

$$Sin(\theta) + \frac{m\lambda}{d} = \sqrt{\frac{\varepsilon' - 1}{\varepsilon'}} \tag{19}$$

The "guided surface wave" must be identified with the SPP of modern literature, since their wavefunctions are the same [9]. The usual expression for the launching of an SPP by a grating is

$$Sin(\theta) + \frac{m\lambda}{d} = \mathrm{Re}\left[\sqrt{\frac{\varepsilon}{1+\varepsilon}}\right] = \frac{c}{\omega} k_{spp} \tag{20}$$

It is interesting to note that the only approximations made to the resonance condition in terms of the relative surface impedance of equation (19) is that $\varsigma'' = -|\varsigma''|$ while Equation (19) is obtained with a more involved set of approximations. Figure 2 shows the expected resonance angle as obtained using the relative surface impedance of Equation (18) minus the expected resonance angle obtained using Equation (19) as a function of $\mathrm{Im}[\varsigma]/\mathrm{Re}[\varsigma]$ at various λ/d ratios. As can be seen, the largest difference is seen as expected at the lower $\mathrm{Im}[\varsigma]/\mathrm{Re}[\varsigma]$ ratios, but even in the extreme case, the angular difference is seen to be less than 0.1degrees.

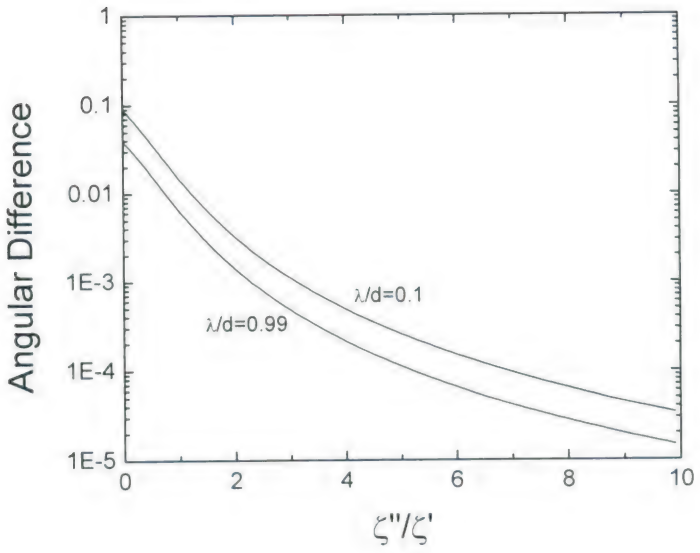

Figure 2: Difference in expected resonance angle obtained using relative surface impedance of Equation (18) minus expected angle obtained using Equation (19) as a function of ζ''/ζ' and λ/d ratios.

For comparison, an alternative perturbation-theory approach to calculating the resonance spectrum was presented by Wheeler et. al. [5]. The resulting formulae are simple in comparison to those of Oliner and Hessel [6]. The reflectivity spectrum for the m = 1 SPP resonance is given by

$$R = \exp\left[-\Delta_1\right] \tag{21}$$

where

$$\Delta_1 = \frac{8\varepsilon''\left(\frac{\pi|\zeta|^2}{\lambda}\right)\left|1-\varepsilon\right|^2 Cos(\theta)\left|2\sigma_1{}^2-\varepsilon\right|\left|\sqrt{2\sigma_1{}^2-1}\sqrt{\left(Sin^2(\theta)-\varepsilon\right)-\sigma_1 Sin(\theta)}\right|^2}{\mathrm{Re}\left[\sqrt{2\sigma_1{}^2-\varepsilon}\right]\left|\sqrt{\left(Sin^2(\theta)-\varepsilon\right)-i\varepsilon\, Cos(\theta)}\right|^2\left|\sqrt{\sigma_1{}^2-\varepsilon}+\varepsilon\sqrt{\sigma_1{}^2-1}\right|^2} \tag{22}$$

with $\sigma_1 = \sin\theta + \lambda / d$, and ζ_1 being the first coefficient of the Fourier transform of the groove profile. Higher harmonics add to Eq. (15) in an obvious way, but we may neglect them since the observed resonances for different m are well separated in our angular spectra.

4. Results

The experiment represented by the Fig. 1 schematic was performed, and out-coupled light was observed with the IR camera when incoming p-polarized light is incident on first grating at the resonance angle determined by Eq. (20) for m=1, which confirms the generation and propagation of an SPP. The light out-coupled at the second grating was found to be highly directional. With the goniometer, it was inconvenient to observe out-coupled corresponding to any other value of m, and these were not looked for. We note that for m = 3, the generated SPP propagates opposite to the direction of the in-plane component of the incident light, and in was experimentally inconvenient to observe out-coupled radiation at a second grating placed to the right of the first (according to Fig. 1). Consequently, generation and propagation of an m=3 SPP was not confirmed, though it is expected. That the generated SPP suffers sufficiently low loss to reach the second grating is supported by the calculated ~1 cm characteristic propagation length for SPPs on noble metals at the CO_2 laser frequency [2].

Fig. 3 (left, inset) presents the measured profile of a 1 micron high Ag grating before and after it was annealed for 30 s at 850 °C. Before annealing, the profile is rectangular. After annealing, the profile has become more sinusoidal except for small bumps on the edges of each line. Fig. 3 (left) presents the Fourier transform of the grating profiles in the inset (including additional periods), with labeled peaks corresponding to the multiples of the fundamental spatial frequency. The as-deposited profile has clear Fourier components up to 6 times the fundamental. The annealed profile has mainly the fundamental, with a small contribution at 5 times the fundamental to account for the bumps on the edges. Notable for the experiments reported here is that the peak corresponding to 3 x the fundamental is strongly attenuated by annealing. Note that the strength of the fundamental is also reduced by annealing.

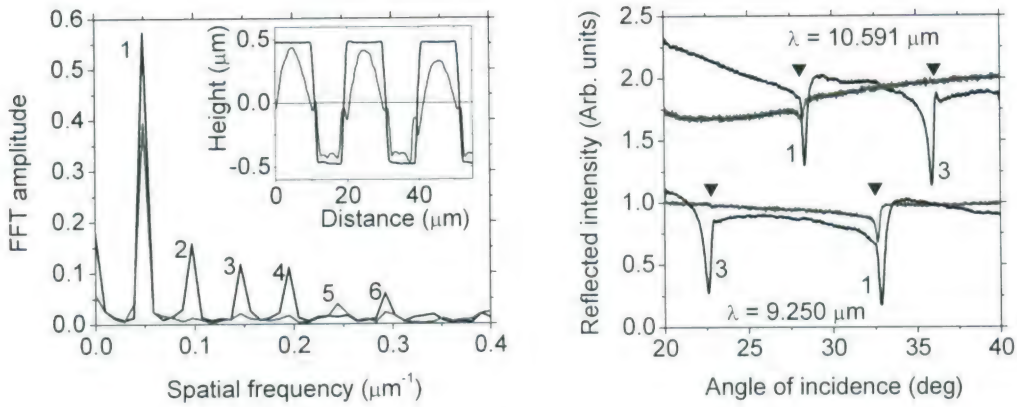

Figure 3 . (left) Fourier transform of measured profiles (inset) for as-deposited and annealed Ag gratings. (right) Angular reflectance spectrum for as-deposited and annealed Ag gratings at two different CO_2 wavelengths.

Fig. 3 (right) presents the reflected intensity as a function of angle of incidence for the 1 micron Ag grating, before and after annealing, for two different wavelengths of the CO_2 laser. Two resonances are observed at each wavelength corresponding to different amounts of grating momentum added to allow generation of a surface plasmon. There is a third resonance predicted near normal incidence, but this is inaccessible to the experiment. Calculated resonance angles θ from Eq. (20), using permittivity values from Table I, are indicated by the symbols. The observed resonances are labeled by the corresponding m value from Eq. (20). The sloping baselines are due to laser power drift, are not repeatable, and can be ignored. The most obvious feature is that the m = 3 resonance nearly disappears from the spectrum for the annealed sample. Second, the m = 1 resonance is reduced in amplitude. Third, the resonance angle undergoes a small shift, with the positions for the annealed sample being closer to the calculated positions.

Fig. 4 (left) presents experimental reflected intensity at two different wavelengths for gratings of different height *h*. For *h* = 100 nm, no absorption resonances were observed. They first appear weakly at *h* = 200 nm, where the m = 1 resonances occur at 32.58 and 28.14 deg for λ = 9.250 and 10.591 μm, respectively. These values are in good agreement with those calculated from Eq. (20) of 32.52 and 28.07 deg with the discrepancy possibly due to systematic error from the estimate of the origin of the angle scale. The resonances are deepest at *h* = 1 μm, but by 2 μm they are strongly

deformed and broadened. As in Fig. 3, the m = 1 and m = 3 resonances switch places when the wavelength is changed from one extreme value of the CO_2 laser range to the other. The m = 1 resonance is always sharpest on the side of low angles, and the baseline of the reflection is lower on that side. For m = 3, the opposite holds.

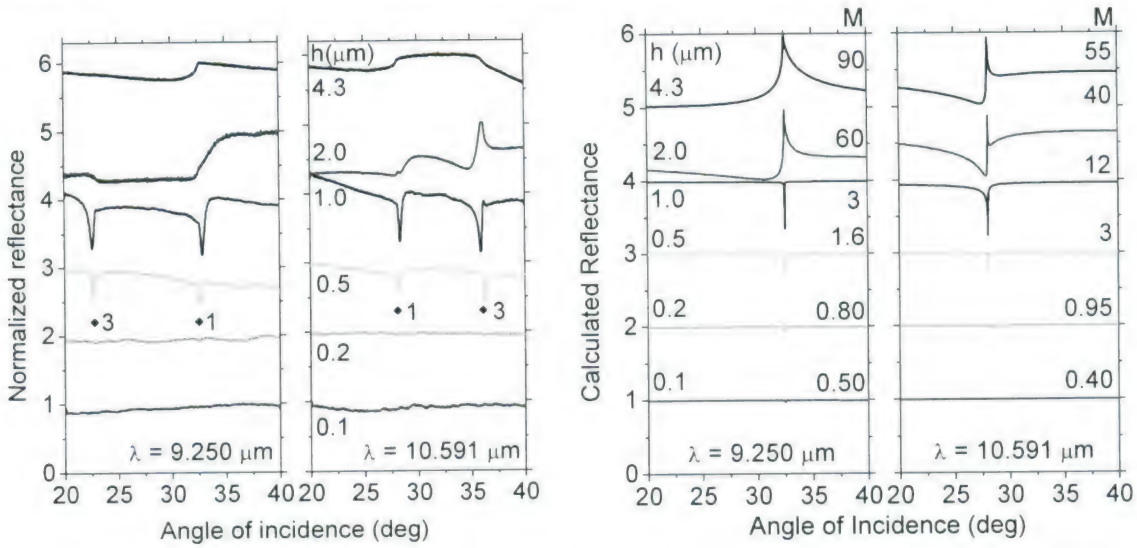

Figure 4 . (left) Measured angular reflectance spectra for two different p-polarized CO_2 laser wavelengths. (right) Calculated spectra from Hessel-Oliner theory.

Figure 4 (right) presents calculated resonance spectra according to the Hessel-Oliner theory, Eq. (11). Since a sinusoidal surface impedance variation is assumed, Eq. (1), with no higher harmonics, we see only the m = 1 resonance, as in Figure 3 for the annealed grating. The observed resonance peaks for the smallest *h* value are 32.52 and 28.07 deg, in exact agreement with the values calculated from Equation (20). The surface impedance modulation amplitude *M* was the only fitting parameter, and its value was adjusted until the calculated curves had the best qualitative agreement with the observed ones. For $h \leq 1$ μm, the depth of the resonance was the main factor in judging the goodness of the fit. For $h > 1$, the lines are distorted, so that other considerations, such as the height of the baseline on either side of the resonance came into play. Notable differences between theory and experiment are in the upward spikes, the line widths, and the absence of any shift in the theoretical resonance positions.

Figure 5 presents the fit values of the surface impedance modulation parameter M as a function of the actual grating height. Error bars were determined by qualitative

assessment of the range of M that adequately matched the observations. For $h \leq 1$ μm, the uncertainty is smaller than the symbol size. For $h > 1$ μm, the distortion of the observed resonances and increasing disagreement between calculated and observed lineshapes leads to larger uncertainty. Two effects are clear in Figure 5. The surface impedance modulation depends non-linearly on grating height, and it has a significant dependence on the optical frequency. Note that the non-linearity appears for smaller values of *h* at the longer wavelength.

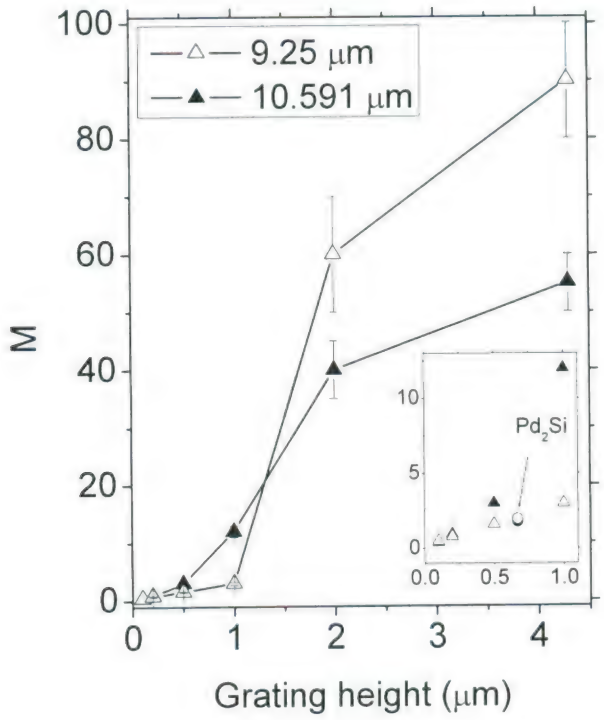

Figure 5 Surface impedance modulation parameter M determined from fit of theory to observed resonances for different grating heights. (Inset) Expanded view of small *h* region with points added from the Pd_2Si experiment.

The observed resonance positions in Figure 4 agree with the calculated values best for the smallest values of *h*. As *h* increases, the resonances shift. The m = 1 lines shift to larger angles with increasing grating height up to $h = 1$ μm, beyond which the line shape is ill defined. The m = 3 lines shift toward smaller angles. We note that the resonances calculated by Hessel-Oliner theory (Figure 4) do not shift. The shifts observed for LWIR in Fig. 4 are compared in Fig. 6 (bottom) to the shifts reported by Heitmann [3] and by Pockrand [4] at visible wavelengths. The shifts appear to be

approximately linear in h up to values of 10% of the wavelength. The shifts at LWIR wavelengths are smaller than for visible wavelengths.

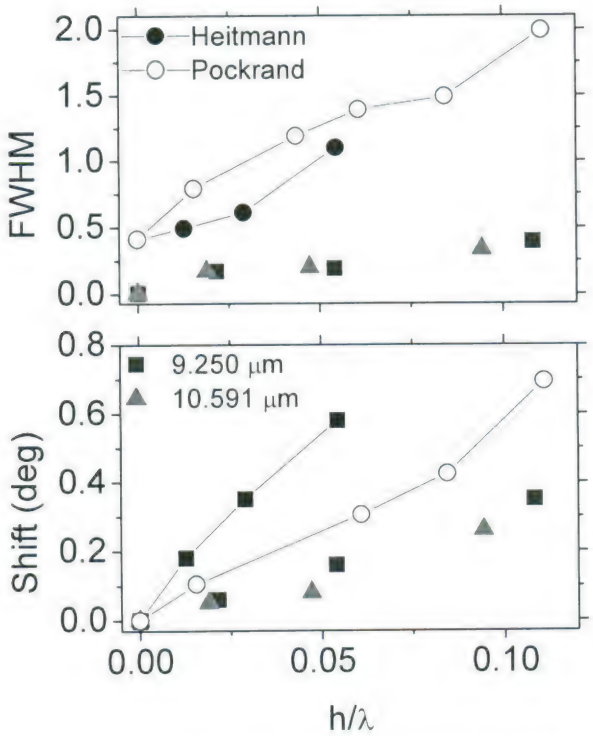

Figure 6 Observed shifts (bottom) and widths (top) of SPP resonances vs. grating height normalized to free space wavelength. The Heitmann [3] and Pockrand [4] data are for λ = 550 nm.

Figure 6 presents the observed widths as a function of grating height for the LWIR m=1 resonance and the widths reported by Heitmann [3] and by Pockrand [4]. Expected widths for h = 0 plotted in Figure 6 are determined from Eq. (3) of Heitmann [3].The angular width is larger in the visible than in the LWIR and increases more rapidly with increasing grating height when plotted against grating height normalized to free space wavelength. These differences will be reduced if the normalization is with respect to the SPP wavelength.

Fig. 7 presents calculated reflectance according to the perturbative approach of [5]. The position of the resonances of 28.07 and 32.52 in the h = 0.1 μm spectrum are in exact agreement with those calculated from Eq. (20). However, the depth of the resonance for this value of h is much greater than observed in Fig. 4 (left). Also, the baseline reflectance rapidly drops toward zero with increasing h, unlike the observation.

Moreover, the resonances line widths are much narrower than observed. As with the Hessel-Oliner theory, there is no shift in the resonance positions as *h* is increased.

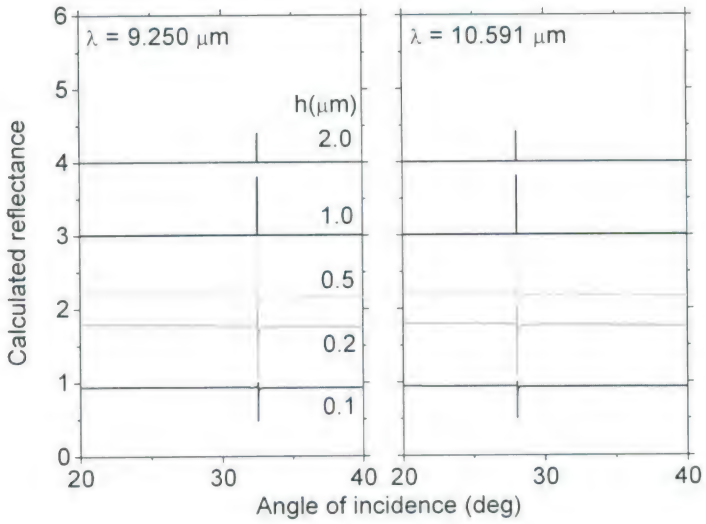

Figure 7 Calculated angular reflectance spectra according to theory of Wheeler, Arakawa, and Ritchie [5]. Traces for successively greater *h* values are shifted vertically by unity.

Figure 8 (left) presents calculated m = 1 resonances at 9.25 μm wavelength from

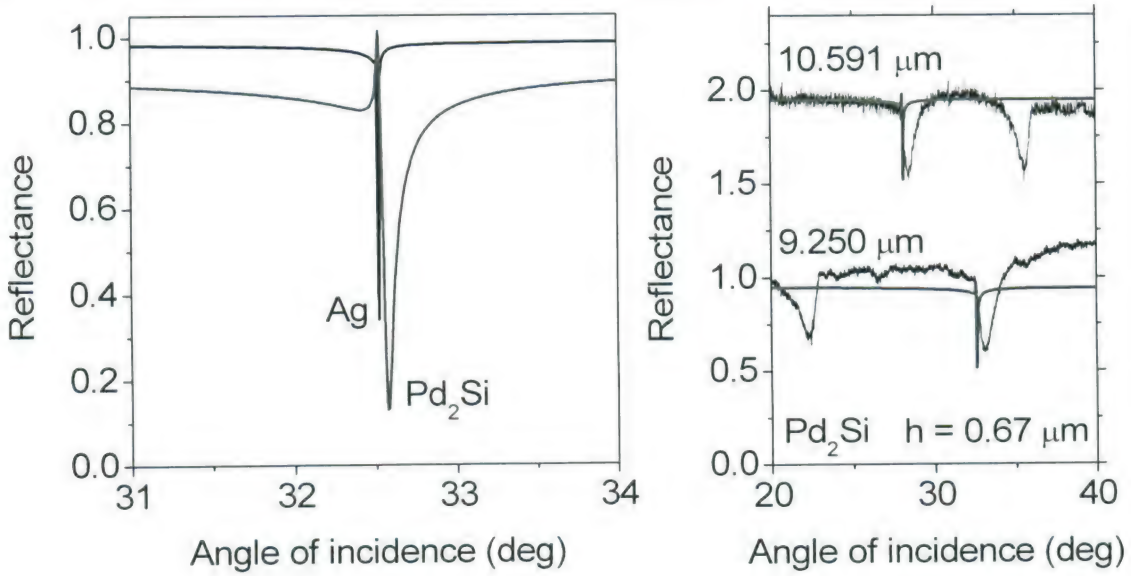

Figure 8 (left) Calculated angular reflectivity spectra from Hessel-Oliner theory for metal and silicide gratings at 9.25 μm wavelength. (right) Measured and calculated angular reflectivity spectra for Pd_2Si grating.

Hessel-Oliner theory and for impedance modulation parameter M = 3, corresponding to h = 1 μm. The high impedance silicide has a deeper broader resonance, indicating that more power is taken out of the optical beam and converted to SPPs.

5. Discussion

From Eq. (20), we have $\mathrm{Sin}\theta = (c/\omega)(k_{SPP} - 2\pi\, m/d) \sim 1 - m\lambda/d$. If the right hand side is positive, as holds for m=1, then an increase in k_{SPP} causes an increase in the resonance angle θ, as observed. If the right hand side is negative, as holds for m = 3, then an increase in k_{SPP} leads to a smaller negative θ, or a smaller positive θ for an SPP traveling in the opposite direction, as observed in Figure 4. Thus, these data indicate that increasing the grating height shifts the SPP dispersion curve toward higher wavenumber, exactly as reported in [3] for e-beam excited SPPs at visible frequencies on sinusoidal Ag gratings.

The shifts in LWIR resonance positions with grating height (Figure 6) are significantly smaller than for visible wavelengths when grating height is normalized to free space wavelength. This is in agreement with [3] that the shift is smaller for the part of the dispersion curve closer to the light line. It suggests that for grating-coupling of monochromatic radiation to SPPs, sensitivity to grating height tolerances will be less in the IR than in the visible.

The linewidth plot in Figure 6 suggests that efficiency of photon-SPP coupling by metal gratings may be better in the IR than in the visible due to deeper sharper resonances, and that this advantage is less sensitive to grating height tolerances. On the other hand, coupling by means of angularly narrow resonances will be more sensitive to angular tolerances.

That relatively low conductivity metal-silicides give deeper broader resonances than noble metals (Figure 8) supports our assertion [2] that these silicon compatible

conductors are interesting for plasmonic applications for the additional reason of efficient photon-SPP coupling.

In conclusion, we have measured the coupling of photons to SPPs by silver or Pd_2Si gratings at CO_2 laser wavelengths and found that the results compare favorable to Hessel-Oliner theory and less well to the Wheeler-Arakawa-Ritchie theory. An empirical non-linear relation between grating groove height and surface-impedance modulation amplitude was found. Stronger photon-SPP coupling was predicted for the higher impedance silicide that for the noble metal, suggesting that these conductors may be preferable for silicon-based IR plasmonic devices. Shifts and broadening of the surface Plasmon resonances with increasing grating height are also reported and found to be weaker than similar effects observed previously at visible wavelengths.

References

1. T. W. Ebbesen, C. Genet, and S. I. Bozhevolnyi, "Surface-plasmon circuitry," Physics Today, May 2008, p.44.
2. R. Soref, R. E. Peale, and W. R. Buchwald, "Longwave plasmonics on doped silicon and silicides," OPTICS EXPRESS 16, 6507 (2008).
3. D. Heitmann, "Radiative decayu of surface plasmons excited by fast electrons on periodically modulated silver surfaces, J. Phys. C: Solid State Phys. 10, 397-405 (1977).
4. I. Pockrand, "Resonance anomalies in the light intensity reflected at silver gratings with dielectric coatings," J. Phys. D: Appl. Phys. 9, 2423 (1976).
5. C. E. Wheeler, E. T. Arakawa, R. H. Ritchie, "Photon excitation of surface plasmons in diffraction gratings: Effect of groove depth and spacing," Phys. Rev. B 13, 2372 (1976).
6. A. Hessel and A. A. Oliner, "A new theory of Wood's anomalies on optical gratings," Appl. Opt. 4, 1275 (1965).
7. Lord Rayleigh, Proc. Roy. Soc. (London) A79, 399 (1907).
8. R. W. Wood, "On a remarkable case of uneven distribution of light in a diffraction grating spectrum," Phil. Mag. 4, 396 (1902).
9. H. Raether, Surface Plasmons on smooth and rough surfaces and on gratings (Springer, Berlin, 1986).

List of Acronyms

IR	infrared
LWIR	long-wave infrared
SSP	surface plasmon polaritons